

## Electronically engineered interface molecular superlattices: STM study of aromatic molecules on graphite

Min Li,<sup>1,\*</sup> Ke Deng,<sup>2</sup> Yan-Lian Yang,<sup>2</sup> Qing-Dao Zeng,<sup>1</sup> Meng He,<sup>2</sup> and Chen Wang<sup>2</sup>

<sup>1</sup>*Institute of Chemistry, Chinese Academy of Sciences (CAS), Beijing 100080, China*

<sup>2</sup>*National Center for Nanoscience and Technology, Beijing 100080, China*

(Received 13 September 2007; published 31 October 2007)

We report the observation of the molecular superlattice driven by the site-dependent adsorption of aromatic molecules on graphite surface by using scanning tunneling microscopy. Furthermore, distinctively different collective assembling characteristics were obtained by introducing coadsorbed molecules or substrate surface charge, revealing the effect of tunable electronic interactions between the molecules and substrate.

DOI: [10.1103/PhysRevB.76.155438](https://doi.org/10.1103/PhysRevB.76.155438)

PACS number(s): 73.21.Cd, 68.65.Cd, 81.16.Dn

Electronic interaction between adsorbed molecules with metallic substrates has been shown to be important in determining the adsorption registry and subsequently assembling behavior.<sup>1</sup> The pressing issue is the nature of the electronic interaction between adsorbed molecules with substrates, which has been shown to be important in determining the adsorption registry.<sup>2</sup> In particular, the family aromatic molecules with  $\pi$  electron characteristics are being extensively pursued, given their high potentials in molecular electronic devices. The *ab initio* calculations<sup>3</sup> clearly indicated that the scanning tunneling microscopy (STM) image of aromatic molecules (such as benzene molecule) is sensitively dependent on the adsorption sites on surfaces, such as graphite. At the same time, it could be noticed that the calculations were only made for the greatly simplified selective sites at bond-centered or hollow sites of the substrate. Previous submolecular resolution STM imaging of benzene molecules on Pt (111) surface<sup>4</sup> and vibrational spectroscopy of benzene adsorbed on Ag (110) (Refs. 5 and 6) provided experimental evidence of the electronic effects on the adsorption of single benzene molecule at special adsorption sites. One should note that these studies were performed on a single molecule level. Such site-dependent adsorption effect of single molecule should also be manifested in the collective assembling characteristics on the molecular assemblies, and yet has never been identified.

The general mechanism that drives the formation of molecular superlattices of aromatic molecules could be finely accommodated by extensive literature on  $\pi$ - $\pi$  interactions between aromatic molecules.<sup>7</sup> The best example can be found in the studies on the stacking behavior of benzene molecule dimers that has been well known to adopt parallel-displaced configuration,<sup>8,9</sup> in which the aromatic molecules adopt cofacial configuration with certain translational displacement of the molecular centers. It was suggested that the specific relative atomic positions for  $\pi$  systems are determined by the  $\pi$ - $\pi$  interaction, and atomic contacts or  $\pi$ - $\sigma$  interaction.<sup>7</sup> Such stacking behavior has been known to play a key role in the formation of molecular nanowires consisted of aromatic molecules. The theoretical analysis, using several different quantum mechanical approaches such as *ab initio* methods, density functional theory, etc., provide the sound ground for the understanding of the displacement behavior reported in this work. On the other hand, graphite has

been well established as the semiconductor with  $\pi$  bands characteristics at the Fermi level, which is formed mainly by the  $p_z$  orbitals.<sup>10-12</sup> It could be plausibly expected that the adsorption of aromatic molecules on graphite surface could be investigated in parallel with the studies on intermolecular interactions between  $\pi$  electrons.

Our experiments demonstrate that the classical effect of  $\pi$ - $\pi$  stacking can be manifested in the molecular adlayer, where both the graphite surface and the adsorbates are known as typical  $\pi$  systems. The evidence was provided on the collective effect due to the mismatch of molecular lattice with substrate lattice in the form of molecular superlattice structures. The observed molecular superlattice demonstrated that, in addition to the topography characteristics of single adsorbed molecule, the electronic interaction between adsorbed molecules with substrates is also important in determining the molecular assembling behavior. The evidences for such adsorption registry have been provided through submolecularly resolved molecular characteristics. Such mismatch of lattice registry could develop into long-range molecular superlattices in the molecular assembling architectures of conjugated  $\pi$  systems.

We investigated an open honeycomb supramolecular network formed by 1,3,5-benzenetricarboxylic acid [trimesic acid, TMA] on highly oriented pyrolytic graphite (HOPG) surface. Normal graphite, as the substrate used in this study, which has a Bernal type with  $D_{6h}^4$  symmetry, consists of layers of a hexagonal network linked by carbon atoms with an *abab* stacking.<sup>13</sup> Graphite surface could also be viewed as an extended conjugated  $\pi$  system which would interact with the introduced molecular adsorbates. During the scanning tunneling microscope (STM) experiment, another assembly network, i.e., “flower” structure, was observed. Such phenomena were also reported in previous studies of TMA assemblies on HOPG surface.<sup>14</sup> Very interestingly, for the honeycomb structure, a hexagonal superlattice with a periodicity of  $58.5 \pm 1.0$  Å was observed in our STM experiments (Fig. 1). However, for the flower-type assembly structure, this superlattice phenomenon could not be observed. It shows a network structure with similar geometry characteristics to that of the substrate is a prerequisite for developing superlattice.

The measured lattice vectors showed that the TMA network rotated by  $(6.0 \pm 0.3)^\circ$  relative to the topmost surface

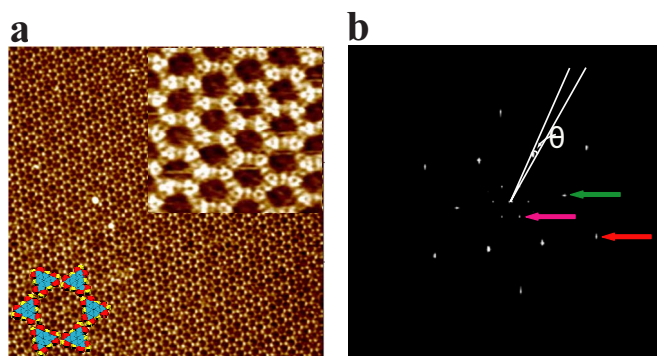


FIG. 1. (Color online) STM image and the corresponding FFT spectrum for TMA network. (a) Constant current STM image ( $63.4 \times 63.4 \text{ nm}^2$ ) of the TMA monolayer on HOPG with the superlattice structure (tunneling conditions:  $I=497 \text{ pA}$ ,  $V=800 \text{ mV}$ ). A proposed model of TMA network is superimposed on the image. Inset: high-resolution image of the assembly structure of TMA adsorbed on HOPG surface. (b) Two-dimensional FFTS of the raw data in (a). The six middle peaks correspond to the TMA network symmetry (pointed out by the green arrow), the six inside peaks to the TMA superlattice symmetry (pointed out by the pink arrow), and the outside peaks to the subperiodicity of TMA networks (pointed out by the red arrow). The angle  $\theta$  in (b) indicates that the TMA superlattice has rotated ( $9.3 \pm 1.0^\circ$ ) relative to the TMA network.

lattice of graphite (Fig. S1 in Ref. 15), while the TMA superlattice is rotated by ( $9.3 \pm 1.0^\circ$ ) relative to the TMA network as shown in Fig. 1(b). The TMA network lattice and the resulted TMA superlattice share the same symmetry which can be observed from the two-dimensional fast Fourier transform spectrum (FFTS) of the STM image [Fig. 1(b)]. The outside peaks in the FFTS correspond to the subperiodicity of TMA networks.

The threefold TMA supramolecular networks connected by the hydrogen bonds could be “locked” to the graphite lattice with the same symmetry and nearly identical lattice constants. Such site recognition is originated from the localized  $\pi$  electron of the phenyl core or so-called “reaction center.” The slight mismatch between the molecular lattice

and atomic graphite lattice is accumulated and compensated by slight adjustment of the hydrogen bond length and angle (Fig. 2), as observed by the periodic and weakly discernible contrast variation in the TMA molecules (Fig. 1). That is, the contrast variation of the molecules is attributed to the variation of hydrogen bond characteristics as the result of the electronic interaction of two structurally similar conjugated  $\pi$  systems represented by adsorbates and substrate, respectively. Such periodic contrast variation of the TMA molecules is manifested in the form of domain structures with characteristic periodicity and rotational angle relative to the molecular lattice. Theoretical calculation<sup>16,17</sup> result of the average TMA-graphite interaction energy is  $36.330 \text{ kJ mol}^{-1}$  (Table SI in Ref. 15) with the associated deviation at different interaction sites (Fig. S2 in Ref. 15) is  $5.015 \text{ kJ mol}^{-1}$  which is ascribed to the local diffusion barrier for the adsorbates, could result in the subtle modulation of the TMA network lattice by graphite for the formation of the superlattice [ $58.5 \pm 1.0 \text{ \AA}$ , ( $9.3 \pm 1.0^\circ$ )].

Furthermore, such adsorbate-substrate electronic interaction could be tuned by introducing coadsorbed molecules. We introduced a coadsorbate to form a binary system in the form of guest-host coupled architecture. The guest molecule modulation on the TMA superlattice was also investigated and coronene (COR) was chosen as the guest molecule. The coronene molecule, which is planar with a sixfold symmetry (space group  $D_{6h}^4$ ), can be considered as the smallest possible flake of a graphite sheet saturated by hydrogen atoms.<sup>18</sup> The cavities within the TMA networks were found to be filled with coronene molecules after adding the dissolved coronene molecules into the predeposited TMA solution on the surface. The commensurability of the adsorbates having structurally similar conjugated  $\pi$  systems with the graphite lattice should be a manifestation of the interactions among the conjugated  $\pi$  systems. Larger hexagonal superlattice can be observed in the STM image with a periodicity of  $93.0 \pm 3.0 \text{ \AA}$  and rotational angle of ( $27.0 \pm 2.5^\circ$ ) relative to the TMA network [Fig. 3(a)]. Both the periodicity and the rotational angle of the superperiodic structure changed significantly in comparison with that of TMA superlattice [ $58.5 \pm 1.0 \text{ \AA}$ , ( $9.3 \pm 1.0^\circ$ )]. The difference can be seen clearly from the

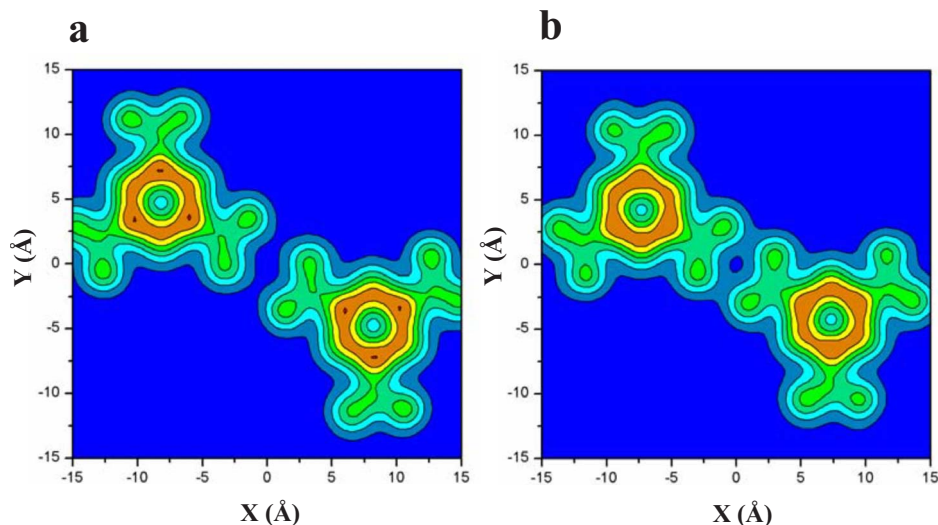


FIG. 2. (Color online) The electron density contour maps of the TMA dimers with different hydrogen bond lengths. (a) The TMA dimer with O-H...O hydrogen bond length about  $2.97 \text{ \AA}$ . (b) The TMA dimer with O-H...O hydrogen bond length about  $2.34 \text{ \AA}$ .

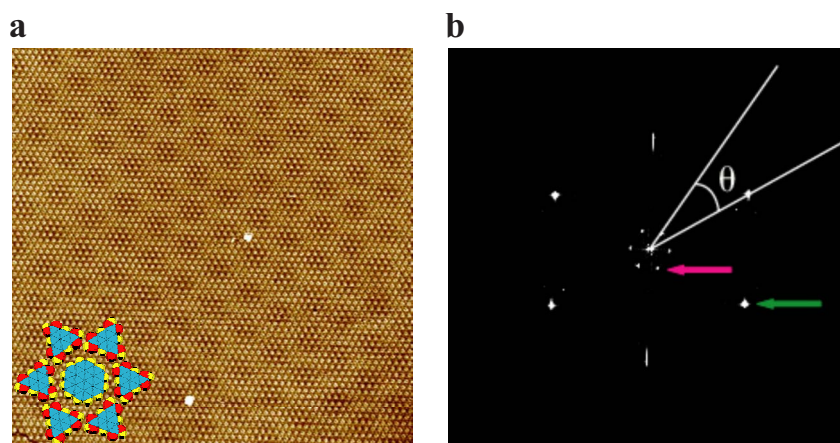


FIG. 3. (Color online) STM image and the corresponding FFT spectrum for COR/TMA network. (a) Constant current STM image ( $100 \times 100 \text{ nm}^2$ ) of the COR/TMA coadsorbed on HOPG with the superlattice structure (tunneling conditions:  $I=745 \text{ pA}$ ,  $V=900 \text{ mV}$ ). A proposed model of COR/TMA assembly is superimposed on the image. (b) Two-dimensional FFTs of the raw data in (a). The six outside peaks correspond to the TMA network symmetry (pointed out by the green arrow) and the six inside peaks to the COR/TMA superlattice symmetry (pointed out by the pink arrow). Note that the COR/TMA superlattice has rotated  $\theta=(27.0 \pm 2.5)^\circ$  relative to the TMA network as shown inside (b).

two-dimensional FFTs of the STM image as shown in Fig. 3(b).

Both the TMA and the COR/TMA architectures have exhibited superlattice structures with similar sixfold symmetry networks (Figs. 1 and 3), which possibly indicate the requirement of the similar symmetry characteristics of molecular networks to that of the substrate for the formation of the molecular superlattice. According to the experiment results and the theoretical calculations,<sup>16,17</sup> the TMA lattice parameters in the COR/TMA architecture ( $16.65 \text{ \AA}$ ) are nearly equal to that of the pure TMA ( $16.57 \text{ \AA}$ ). It indicates that the formation of the superlattice was not due to the periodicity variations of the TMA network. The theoretical calculations

suggested a very small deviation energy ( $3.956 \text{ kJ mol}^{-1}$ ) when COR interacts with the graphite lattice as shown in Table SI in Ref. 15. Such little deviation cannot be the driving force for the formation of the superlattice. In addition, the TMA lattice in the COR/TMA architecture is rotated relative to the topmost graphite surface by  $(5.4 \pm 0.5)^\circ$  as shown in Fig. S3 in Ref. 15, in agreement with that of the TMA network [ $(6.0 \pm 0.3)^\circ$ ] without the COR molecules. It implies that the superlattices mentioned above are not due to the rotational misorientation between adsorbates and substrate layers.

It is evident that the COR/TMA superlattice can be better resolved with a larger rotation angle [ $(27.0 \pm 2.5)^\circ$ ] than that

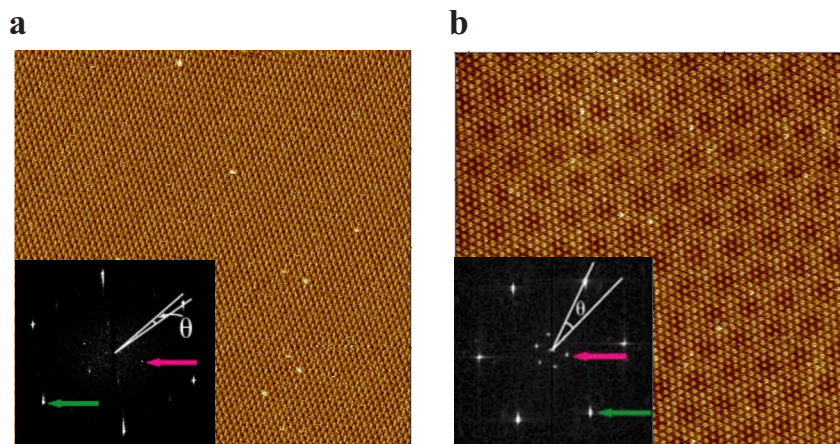


FIG. 4. (Color online) STM images and the corresponding FFT spectrum for both TMA and COR/TMA systems with +4000 V application. Constant current STM images of the (a) TMA ( $100 \times 100 \text{ nm}^2$ ) and (b) COR/TMA ( $77.5 \times 77.5 \text{ nm}^2$ ) on HOPG with the superlattice structure after applying +4000 V to the substrate for about 1.5 h. (a) Tunneling conditions:  $I=617 \text{ pA}$ ,  $V=640 \text{ mV}$ . Inset: two-dimensional FFTs of the raw data in (a). The six outside peaks correspond to the TMA network symmetry (pointed out by the green arrow) and the six inside peaks to the TMA superlattice symmetry (pointed out by the pink arrow). The angle  $\theta$  indicates that the TMA superlattice has rotated  $(5.3 \pm 1.0)^\circ$  relative to the TMA network. (b) Tunneling conditions:  $I=742 \text{ pA}$ ,  $V=800 \text{ mV}$ . Inset: FFTs of the raw data in (b). The six outside peaks correspond to the TMA network symmetry (pointed out by the green arrow) and the six inside peaks to the COR/TMA superlattice symmetry (pointed out by the pink arrow). Note that the COR/TMA superlattice has rotated  $\theta=(19.6 \pm 0.8)^\circ$  relative to the TMA network.

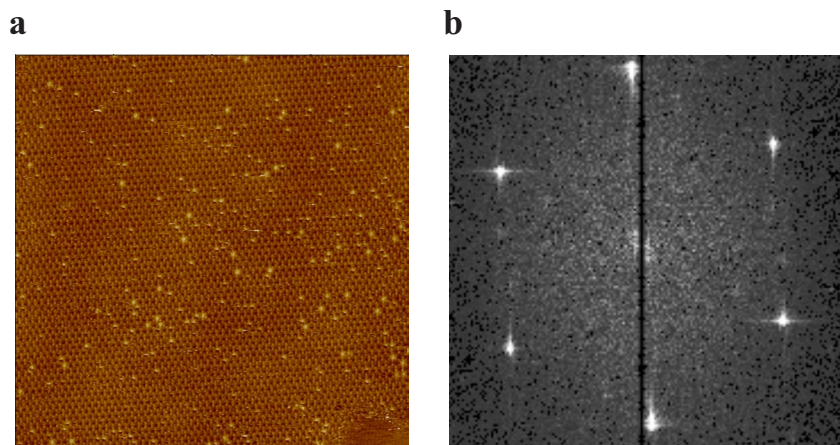


FIG. 5. (Color online) STM image and the corresponding FFT spectrum for TMA systems with  $-4000$  V application. (a) Constant current STM image ( $100 \times 100$  nm<sup>2</sup>) of the TMA on HOPG after applying  $-4000$  V to the substrate for about 1.5 h (tunneling conditions:  $I = 739$  pA,  $V = 560$  mV). (b) Two-dimensional FFTs of the raw data in (a). The six peaks correspond to the TMA network symmetry and the six inside peaks corresponded to TMA superlattice symmetry nearly disappeared.

of the TMA superlattice (Figs. 1 and 3). We attribute this observation to the modulation of the electronic structures resulted from the interaction of adsorbates with substrate. The electronic structure of the substrate can be perturbed by the presence of the adsorbed molecule electrons, and vice versa.<sup>1,19–22</sup>

The introduction of coadsorbed molecules is accompanied by the additional electronic interactions between molecules and substrate. The coadsorbed coronene molecules, having nearly the same atomic structure as the graphite lattice, also tend to lock to the underlying graphite lattice due to the same site recognition mechanism of reaction centers associated with localized  $\pi$  electrons. Consequently, the mismatch between TMA supramolecular lattice and graphite lattice is compensated with differed characteristics due to the existence of the coadsorbed coronene molecules within the molecular lattice.

Further experiments were carried out by introducing surface charge to the substrate through applying an external voltage to the substrate to change the electronic interaction of adsorbate-graphite system. When positive voltage ( $+4000$  V) was introduced to the substrate, both the TMA and COR/TMA superlattices displayed a similar trend of variations, that is, the superlattice periodicities and rotational angles shown in Fig. 4 are appreciably reduced as compared with that of the systems without applied voltage to the substrate [for TMA superlattice:  $58.5 \pm 1.0$  Å,  $(9.3 \pm 1.0)^\circ$  (for  $V_{\text{substrate}} = 0$  V) to  $50.0 \pm 3.0$  Å,  $(5.3 \pm 1.0)^\circ$  (for  $V_{\text{substrate}} = +4000$  V); for COR/TMA superlattice: to  $93.0 \pm 3.0$  Å,  $(27.0 \pm 2.5)^\circ$  (for  $V_{\text{substrate}} = 0$  V) to  $74.0 \pm 1.5$  Å,  $(19.6 \pm 0.8)^\circ$  (for  $V_{\text{substrate}} = +4000$  V)]. It implies that increasing the posi-

tive charges on the substrate would enhance the charge transfer from adsorbate to substrate which results in the increased local diffusion barrier and consequently decrease the superlattice parameters. When negative voltage ( $-4000$  V) was applied to the substrate, the charge transfer from adsorbate to substrate was hampered, which significantly reduced the local diffusion barrier and therefore the adsorbate-substrate electronic interaction. As a result, the superlattice phenomenon of TMA network nearly disappeared [Fig. 5(b)]. However, for the COR/TMA system, the electronic adsorbate-graphite interaction was not counteracted due to the strong interaction of COR/TMA with graphite. These observations further demonstrated that the molecular superlattices were formed by adsorbate-substrate electronic interaction and could be modulated through varying such electronic interaction.<sup>15</sup>

Our results show that the molecular superlattice was driven by the site-dependent adsorption effect due to electronic interactions between the molecules and substrate. Such interaction could be further tuned by introducing coadsorbates or substrate surface charge. These results manifested the significance of electronic interactions in engineering molecular interfaces in complementary to the previously reported registration effects of single molecules.<sup>23–26</sup>

#### ACKNOWLEDGMENTS

Financial support from National Natural Science Foundation of China (90406019 and 20473097) is gratefully acknowledged. Chinese Academy of Sciences (CAS) and the Ministry of Science and Technology (MOST) are also appreciated for the financial support.

\*Also at CAS Graduate School, Beijing 100049, China.

- <sup>1</sup>M. Eremtchenko, J. A. Schaefer, and F. S. Tautz, *Nature (London)* **425**, 602 (2003).
- <sup>2</sup>P. Sautet, *Chem. Rev. (Washington, D.C.)* **97**, 1097 (1997).
- <sup>3</sup>A. J. Fisher and P. E. Blochl, *Phys. Rev. Lett.* **70**, 3263 (1993).
- <sup>4</sup>P. S. Weiss and D. M. Eigler, *Phys. Rev. Lett.* **71**, 3139 (1993).
- <sup>5</sup>J. I. Pascual, J. J. Jackiw, K. F. Kelly, H. Conrad, H.-P. Rust, and P. S. Weiss, *Phys. Rev. B* **62**, 12632 (2000).
- <sup>6</sup>J. I. Pascual, J. J. Jackiw, Z. Song, P. S. Weiss, H. Conrad, and H.-P. Rust, *Phys. Rev. Lett.* **86**, 1050 (2001).
- <sup>7</sup>C. A. Hunter and J. K. M. Sanders, *J. Am. Chem. Soc.* **112**, 5525 (1990).
- <sup>8</sup>E. G. Cox, *Rev. Mod. Phys.* **30**, 159 (1958).
- <sup>9</sup>R. L. Jaffe and G. D. Smith, *J. Chem. Phys.* **105**, 2780 (1996).
- <sup>10</sup>P. R. Wallace, *Phys. Rev.* **71**, 622 (1947).
- <sup>11</sup>J. C. Slonczewski and P. R. Weiss, *Phys. Rev.* **109**, 272 (1958).
- <sup>12</sup>N. A. W. Holzwarth, S. G. Louie, and S. Rabii, *Phys. Rev. B* **26**, 5382 (1982).
- <sup>13</sup>P. J. Ouseph, *Phys. Rev. B* **53**, 9610 (1996).
- <sup>14</sup>S. Griessl, M. Lackinger, M. Edelwirth, M. Hietschold, and W. M. Heckl, *Single Mol.* **3**, 25 (2002).
- <sup>15</sup>See EPAPS Document No. E-PRBMDO-76-097739 for a presentation of the sample preparation process. For more information on EPAPS, see <http://www.aip.org/pubservs/epaps.html>.
- <sup>16</sup>J. P. Perdew and Y. Wang, *Phys. Rev. B* **45**, 13244 (1992).
- <sup>17</sup>A. D. Becke, *J. Chem. Phys.* **88**, 2547 (1988).
- <sup>18</sup>W. W. Duley and S. S. Seahra, *Astrophys. J.* **522**, L129 (1999).
- <sup>19</sup>D. R. Clarke, M. Kuwabara, and D. A. Smith, *Appl. Phys. Lett.* **56**, 2396 (1990).
- <sup>20</sup>Z. Y. Rong and P. Kuiper, *Phys. Rev. B* **48**, 17427 (1993).
- <sup>21</sup>Y. Zou, L. Kilian, A. Scholl, Th. Schmidt, R. Fink, and E. Umbach, *Surf. Sci.* **600**, 1240 (2006).
- <sup>22</sup>M. Ruben, D. Payer, A. Landa, A. Comisso, C. Gattinoni, N. Lin, J.-P. Collin, J.-P. Sauvage, A. De Vita, and K. Kern, *J. Am. Chem. Soc.* **128**, 15644 (2006).
- <sup>23</sup>R. Hentschke, B. L. Schurmann, and J. P. Rabe, *J. Chem. Phys.* **96**, 6213 (1992).
- <sup>24</sup>A. Stabel, R. Heinz, J. P. Rabe, G. Wegner, F. C. De Schryver, D. Corens, W. Dehaen, and C. Sueling, *J. Phys. Chem.* **99**, 8690 (1995).
- <sup>25</sup>J. P. Rabe, S. Buchholz, and L. Askadskaya, *Synth. Met.* **54**, 339 (1993).
- <sup>26</sup>J. P. Rabe and S. Buchholz, *Science* **253**, 424 (1991).